X-ray structural characterization, Raman and thermal analysis of $LiNH_4SO_4$ above room temperature

1999 J. Phys.: Condens. Matter 11 8995

(http://iopscience.iop.org/0953-8984/11/46/303)

J. Phys.: Condens. Matter **11** (1999) 8995–9007. Printed in the UK PII: S0953-8984(99)03914-4

X-ray structural characterization, Raman and thermal analysis of $LiNH_4SO_4$ above room temperature

Xavier Solans, Jorge Mata, M Teresa Calvet and Mercè Font-Bardia

Departament Cristallografia, Mineralogia i Dipòsits Minerals, Universitat de Barcelona, E-08028-Barcelona, Spain

Received 4 May 1999, in final form 8 September 1999

Abstract. Results are presented of a detailed x-ray diffraction, Raman and thermal analysis study of the structural phase transitions in $LiNH_4SO_4$ carried out in the temperature range 298–600 K. Either two or just one phase transition was recorded in the temperature range between 335 and 461 K, depending on the warming process rate. Crystal structures at 298, 318, 383, 423 and 483 K during a slow warming process and at 298 and 523 K during a fast warming process were solved. The transition at 335 K is reported for the first time and consists of a rotation by 41° of the sulphate ion around an S–O bond. The new obtained phase above 335 K is close to the enantiomeric phase at room temperature. The high temperature phase crystallized in the non-polar $P2_1nb$ space group, but the crystal structure obtained removed the spontaneous polarization, according to the calculations made using an ionic model, and agrees with the experimental results.

1. Introduction

The phase transition sequence displayed by $LiNH_4SO_4$ (LAS) above room temperature has been extensively studied in recent years but a definitive picture has yet to be obtained. Interest in this compound is derived from its ferroelastic and ferroelectric properties and the identification of several phase transitions in the temperature range 10 to 615 K. According to the literature [1–3] the paraelectric phase at high temperature (phase I) undergoes a phase transition at 460 K to the ferroelectric phase II which in turn undergoes a transition to ferroelastic phase III at 285 K. Dollase [4] determined the structure at room temperature as being orthorhombic, with the space group $P2_1nb$ and four formulae in the unit cell. This structure was subsequently refined by Mashiyama and Kasano [5]. Itoh *et al* [2] solved the structure of the paraelectric phase at 478 K. It is also orthorhombic, with the space group *Pmnb*. Polomska *et al* [6] observed a DTA maximum at about 350 K, which was related to an irreversible transformation from phase I to phase II. Torgashev *et al* [7] observed an anomalous behaviour of Raman spectra at high temperatures (above 460 K) when the space group was assigned as *Pmnb* and they accounted for this by indicating the presence of orientational disorder in the *Pmnb* phase. Here, in order to elucidate and to characterize the phase transition of LAS, a thermal, Raman and x-ray diffraction study was carried out.

0953-8984/99/468995+13$30.00

Table 1. Crystal data and structure refinement for $LiNH_4SO_4$ at different temperatures.

Data for all structures						
Empirical formula	$LiNH_4SO_4$					
Formula weight	121.04					
Wavelength (Å)	0.710 69					
Crystal system, space group	orthorhombic, $P2_1nb$					
Z	4					
$F(000)$	248					
Crystal size (mm)	$0.2 \times 0.2 \times 0.4$					
θ range (°) for data collection	3.22 to 29.96					
Index ranges	$0 \leqslant h \leqslant 7, 0 \leqslant k \leqslant 12, 0 \leqslant l \leqslant 12$					
	Phase II	Phase II + II′	Phase II + II′	Phase II′	Phase I′	Phase I
Temperature (K)	298.0(2)	318.0(2)	383.0(2)	423.0(2)	483.0(2)	523.0(2)
a (Å)	5.276(4)	5.279(3)	5.302(6)	5.304(4)	5.304(3)	5.292(9)
b (Å)	8.768(3)	8.775(3)	8.780(2)	8.782(2)	8.774(2)	8.769(7)
c (Å)	9.122(2)	9.122(2)	9.140(2)	9.1466(14)	9.1661(11)	9.198(3)
Volume (Å^3)	422.0(4)	422.6(3)	425.5(5)	426.0(3)	426.6(3)	426.8(8)
ρ (Mg m^{-3})	1.905	1.903	1.890	1.887	1.885	1.884
μ (mm^{-1})	0.651	0.650	0.645	0.644	0.644	0.643
Reflec. collected/unique	654/654	1296/669	698/651	668/668	668/662	659/659
Completeness to 2θ	96.7%	98.7%	95.4%	97.4%	96.6%	96.1%
Data/parameters	654/77	660/78	651/82	668/80	662/80	659/77
S	1.122	1.078	1.142	1.188	1.095	1.101
R_1 index (all data)	0.0376	0.0364	0.0439	0.0494	0.0500	0.0783
wR_2 index (all data)	0.1144	0.1008	0.1046	0.1166	0.1225	0.2172
Flack parameter	0.1(3)	0.0(2)	0.0(5)	0.0(3)	−0.3(4)	0.6(6)
Phase II/(Phase II + II′) rate	1.00	0.874	0.118	0.00	—	—
Extinction coefficient	0.002(9)	0.04(8)	0.99(9)	0.61(7)	0.45(5)	0.14(4)
Largest diff. peak (e Å^{-3})	0.613	0.451	0.455	0.672	0.844	1.220

2. Experimental section

2.1. Synthesis and crystallization

The LAS was obtained via the reaction of $(NH_4)_2SO_4$ with $Li_2SO_4.H_2O$ in aqueous solution at 333 K. The molar ratio between the ammonium and lithium sulphates was 1:1, 1.5:1 and 2:1. Crystals were grown by slow evaporation at 333 K. An increase in the ammonium ratio decreased the growth velocity. The best phase II crystals were obtained with the ratio 1.5:1. The compound obtained was analysed by ICP (induced condensed plasma) with a Jobin–Yvon analyser and x-ray powder diffraction.

2.2. Thermal analysis

The thermal analysis for the temperature range 293–600 K was carried out in a differential scanning calorimeter (DSC) Perkin–Elmer DSC-7. The warming rate was 5 K min^{-1} and 20 K min^{-1} and the sample weight was 12.66 mg.

2.3. X-ray structure determination

A similar method was followed in all single-crystal structure determinations, where the same crystal was used in all measurements. The intensities were measured at the constant temperatures of 298, 318, 383, 423 and 483 K, applying a warming rate of 5 K min^{-1}. The crystal was cooled to 298 K and intensity data were recorded. Subsequently, the crystal was warmed at a faster rate (20 K min^{-1} rate) at and the intensity data were recorded at 523 K. Diffraction data were collected on an Enraf–Nonius CAD4 automated diffractometer equipped with a graphite monochromator. The ω–2θ scan technique was used to record the intensities. Scan widths were calculated as $A + B\tan\theta$, where A is estimated from the mosaicity of the crystal and B allows for the increase in peak width due to Mo Kα_1–Kα_2 splitting.

Table 2. Equivalent isotropic displacement parameters (Å$^2 \times 10^3$) at different temperatures, which are compared with the values at 478 K obtained by Itoh *et al* [2] (* = atoms with an occupancy factor equal to 0.5). U(eq) is defined as one third of the trace of the orthogonalized U_{ij} tensor.

	$T = 298.0$ K	$T = 318.0$ K	$T = 383.0$ K	$T = 423.0$ K	$T = 483.0$ K	$T = 523.0$ K	$T = 478.0$ K
S	22(1)	17(1)	20(1)	22(1)	25(1)	34(1)	34(1)
O(1)	41(1)	63(1)	73(1)	80(2)	97(2)	114(4)	126 (3)*
O(2)	39(1)	47(1)	57(1)	63(1)	76(1)	98(3)	76(1)*
O(3)	33(1)	37(1)	40(1)	44(1)	51(1)	82(3)	111(2)*
O(4)	31(1)	33(1)	45(1)	49(1)	59(1)	71(2)	67(1)*
N	26(1)	29(1)	35(1)	38(1)	43(1)	52(1)	54(1)
Li	18(1)	23(1)	27(1)	30(1)	33(1)	42(2)	44(1)

Details of structure determination are listed in table 1. The unit-cell parameters were obtained by a least-squares fit to the automatically centred settings from 25 reflections ($12^\circ < 2\theta < 21^\circ$). The intensities from three control reflections for each measurement showed no significant fluctuation during data collection.

The structures were solved by direct methods, using the SHELXS-97 computer program [8] and refined by the full-matrix least-squares method, using the SHELXL-97 computer program [9]. The function minimized was $w||F_0|^2 - |F_c|^2|^2$, where the weighting scheme was $w = [\sigma^2(I) + (k_1P)^2 + k_2P]^{-1}$ and $P = (|F_0|^2 + 2|F_c|^2)/3$. The values of k_1 and k_2 were also refined. The chirality of the structure was defined from the Flack coefficient [10].

Refinements assuming the possible mixture of different phases were carried out on all intensity data collected. The crystal structures at 483 and 523 K were solved by direct methods in both space groups $P2_1nb$ and *Pmnb*. The positions of all non-hydrogen atoms were obtained using the $P2_1nb$ space group, though the structure was not solved when the *Pmnb* space group was used. Refinements were made to these structures in both space groups, using the average positions obtained in the non-centrosymmetric group for the centrosymmetric space group and assuming the oxygen and hydrogen atoms to lie in disorder sites. The results obtained with the *Pmnb* group were in agreement with those obtained by Itoh *et al* [2], with larger equivalent isotropic thermal parameters for disorder atoms with an occupancy factor equal to 0.5 (table 2). Refinements assuming the contribution to intensity as coming partially from the non-centrosymmetric coordinates and partially from those equivalent by a mirror plane to the previous values (as if the crystal were a twin crystal) did not converge at 523 K and gave a contribution equal to 100% for the assumed enantiomer at 483 K. The lower R value, lower density in the maximum peak in the final difference map and the lower Flack parameter indicate that the correct solution at 483 and 523 K is obtained by using the non-polar group. The poorer results obtained at 523 K can be explained by defective growth produced by the dilatation and

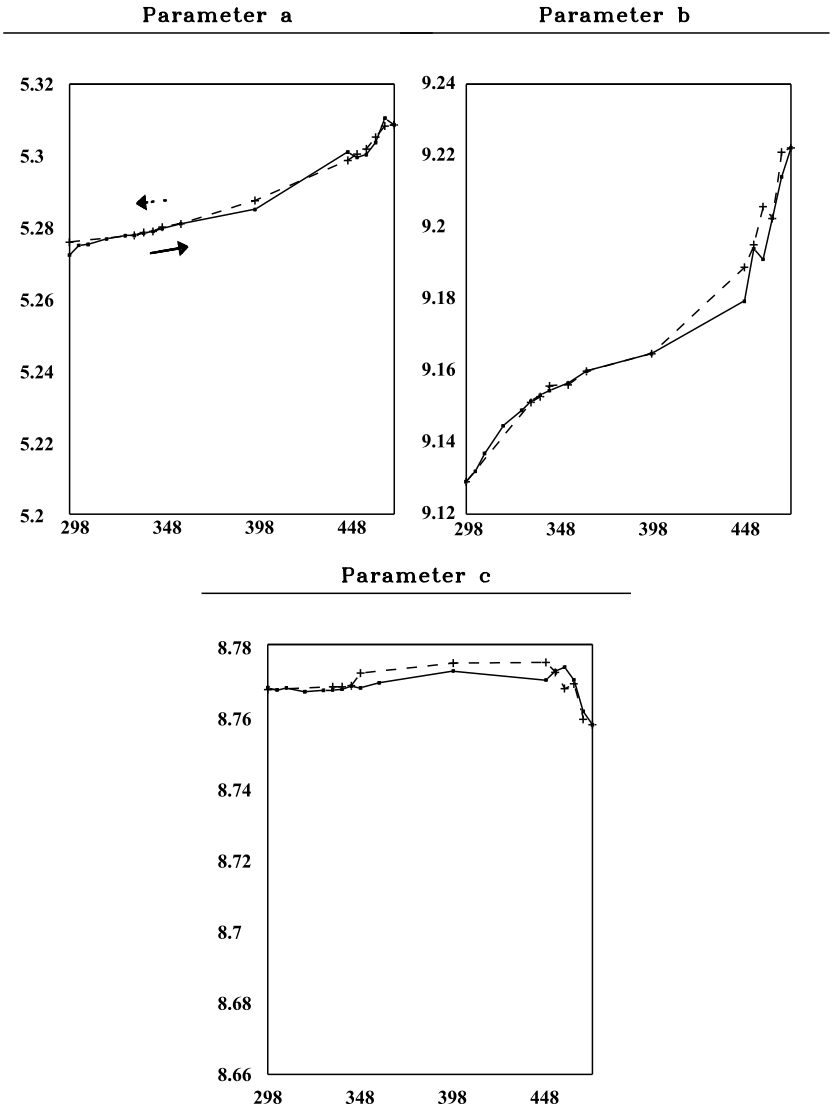

Figure 1. Variation of the cell parameters versus the temperature for $LiNH_4SO_4$.

contraction of crystal after undergoing the two warming and the cooling processes, in particular the fast warming process.

Hydrogen atoms were located in all crystal structure determinations from a difference map, and were refined with the N–H bond length constrained to 0.95 Å.

2.4. X-ray powder diffraction

Powder-diffraction data were collected with a Siemens D500 at different temperature, using Cu Kα radiation and a secondary monochromator. The experiment was a warming process from 298 to 500 K followed by a cooling process between the same temperatures. The cooling and warming rates were 5 K min^{-1} and the sample was left for 10 min. At measuring temperature

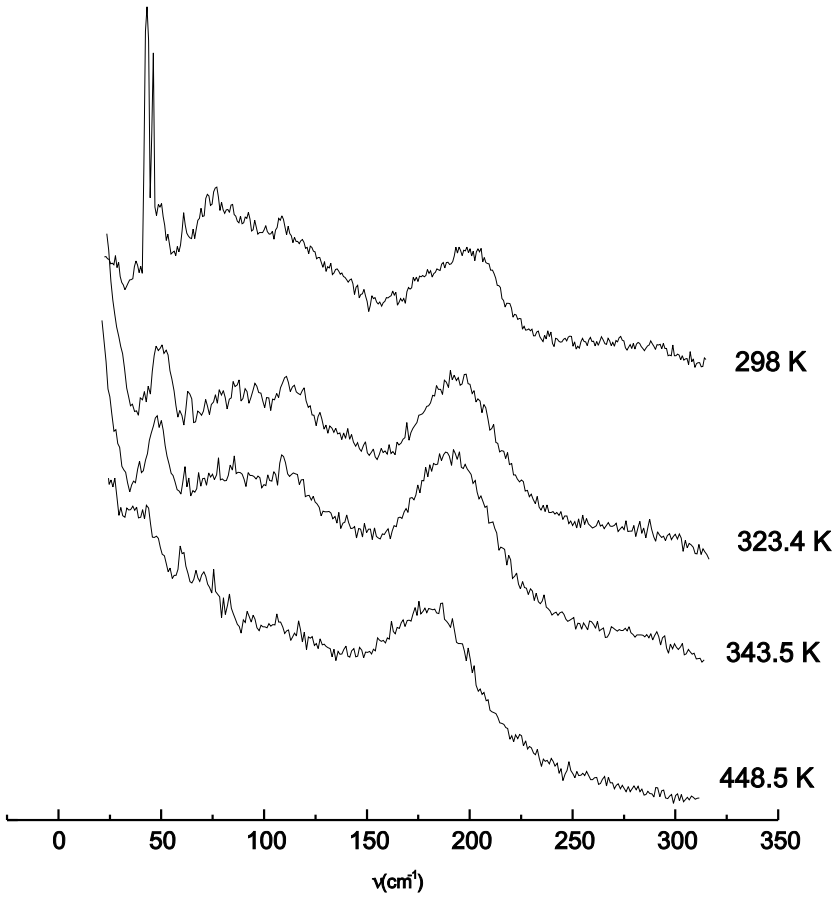

Figure 2. External modes of Raman spectra of LAS at different temperatures.

in order to stabilize the equipment and the sample. The step size was 0.025°, the time of each step 10 s, and the 2θ range was 10–80°. Cell parameters (figure 1) from powder diffraction were refined with the FULLPROF computer program [11].

2.5. Raman scattering

Polarized Raman spectra were excited on the powder sample using a Jobin–Yvon T64000 spectrometer, and an argon-ion laser excitation. The detector used was a Control Data CDC. The spectra were recorded with three monochromator gratings and the 514.5 nm line was used with a light power equals to 1.05 W. All spectra were calibrated against selected neon lines. A Mettler FP84 sample warming cell was used in order to measure the spectra at different temperatures. The position, half width and relative intensity of each peak (table 3) was determined, assuming it to be a Lorentzian function (the Gaussian contribution is negligible).

3. Results and discussion

The DSC revealed two maxima at 335 and 461 K when the warming rate was 5 K min^{-1}. Thus, the maximum described by Polomska *et al* [6] was observed, but the 335 K maximum was not

Table 3. Frequencies (in cm^{-1}), half-width and integrated area of phonon modes in LAS at different temperatures.

	$T = 298$ K	$T = 323.4$ K	$T = 343.5$ K	$T = 448.5$ K
t^{SO_4}	41.14(7)	43.2(4)	44.2(4)	31.7(6)
	3.4(2)	37(2)	31(2)	66(4)
	172	1085	959	406
t^{SO_4}	76.5(18)	78.9(12)	76.1(13)	71.7(6)
	107(5)	25(7)	31(8)	26(4)
	3385	213	355	263
L^{SO_4}	118.3(17)	108(2)	108(2)	110.9(11)
	21(9)	70(5)	73(6)	102(6)
	117	1818	1912	2890
t^{NH_4}	195.2(6)	190.4(4)	190.2(5)	183.1(2)
	39(3)	48.7(16)	59.9(19)	56.2(11)
	761	1480	1907	2026
t^{Li}	366(2)	362(3)	367(3)	
	44(23)	18(21)	32(31)	
	169	20	65	
t^{Li}	394.6(8)	394.4(11)	391.6(10)	
	16(5)	19(8)	18(6)	
	77	85	94	
$\nu_2^{SO_4}$	463.9(7)	463.8(5)	469.35(19)	465.13(7)
	27.2(8)	23.2(8)	30.8(6)	25.5(2)
	4748	2415	6145	5161
$\nu_2^{SO_4}$	475.1(7)	474.71(15)		
	11(3)	14.7(5)		
	497	2143		
$\nu_4^{SO_4}$	633.2(12)	632.93(12)	634.6(3)	634.01(12)
	27(1)	16.5(3)	22.2(8)	23.0(4)
	2252	2764	2468	2581
$\nu_4^{SO_4}$	642.3(6)	645.80(17)		
	9(3)	9.3(6)		
	421	445		
$\nu_1^{SO_4}$	1007.83(3)	1008.67(1)	1008.78(2)	1006.978(13)
	6.93(8)	8.19(3)	8.43(5)	12.43(4)
	5493	5743	5301	5440
$\nu_3^{SO_4}$	1086.6(3)	1090.4(3)	1090.8(3)	
	16.8(10)	11.6(15)	10.3(13)	
	374	208	153	
$\nu_3^{SO_4}$	1104.86(8)	1105.6(4)	1105.3(3)	1103(4)
	14.2(4)	27.8(10)	27.7(7)	47.1(10)
	1217	1393	1320	2216
$\nu_3^{SO_4}$	1121.6(3)			
	14.6(12)			
	327			

Table 3. (Continued)

	$T = 298$ K	$T = 323.4$ K	$T = 343.5$ K	$T = 448.5$ K
$\nu_3^{SO_4}$	1149.9(4)	1148.20(19)	1148.13(17)	1145.0(4)
	29.3(14)	24.4(8)	25.2(7)	30.9(19)
	677	1155	1068	1114
$\nu_3^{SO_4}$	1175.0(5)	1174.8(4)	1180.5(9)	
	20.2(22)	19.1(17)	54(2)	
	440	385	1502(79)	
$\nu_3^{SO_4}$	1192.7(2)	1191.9(3)	1191.8(2)	
	15.9(6)	16.0(9)	14.7(7)	
	419	524	386	
$\nu_4^{NH_4}$	1408.70(8)	1412.4(8)		
	25.2(3)	31(2)		
	641	371		
$\nu_4^{NH_4}$	1441.5(8)	1438.5(7)	1431.2(5)	1435.1(9)
	55.4(16)	37.0(16)	69(2)	98(3)
	382	647	1438	1410
$\nu_2^{NH_4}$	1646(2)	1645(4)		
	60(5)	71(7)		
	618	548		
$\nu_2^{NH_4}$	1680.55(17)	1680.9(2)	1678.4(2)	1674.6(5)
	28.3(7)	31.4(10)	50.4(8)	86.8(16)
	1590	1336	1967	1951
$\nu_1^{NH_4}$	2855.9(9)	2855(3)	2848(2)	2848(6)
	80(3)	72(9)	125(6)	293(13)
	1275	1168	2123	3405
$\nu_1^{NH_4}$	3051.6(4)	3044.8(13)	3048(1)	3058(2)
	123.0(16)	121(5)	145(4)	162(9)
	7925	8099	8457	6783
$\nu_3^{NH_4}$	3186.0(9)	3176(2)	3181.9(11)	3185.4(13)
	185(2)	153(5)	160(3)	154(3)
	10000	10000	10000	10000

observed when the warming rate was 20 K min^{-1}. This suggests that LAS might undergo two phase transitions in the temperature range studied (293–600 K). The ΔH (J mol^{-1}) were 119 and 610 for the transitions at 335 and 461 K, respectively and the ΔT (difference between the initial and final onset temperatures) were 17.7 and 6.2 K, respectively. The melting point was 601 K.

5 K min^{-1}

$$\text{Phase II} \xrightarrow{335\ \text{K}} \text{Phase II}' \xrightarrow{461\ \text{K}} \text{Phase I}' \xrightarrow{601\ \text{K}} \text{Melt}$$

20 K min^{-1}

$$\text{Phase II} \xrightarrow{461\ \text{K}} \text{Phase I} \xrightarrow{601\ \text{K}} \text{Melt}.$$

The two transitions were confirmed by x-ray powder diffraction. At 461 K the transition is observed by means of an abrupt change in the values of *b* and *c* parameters (figure 1). The *a*

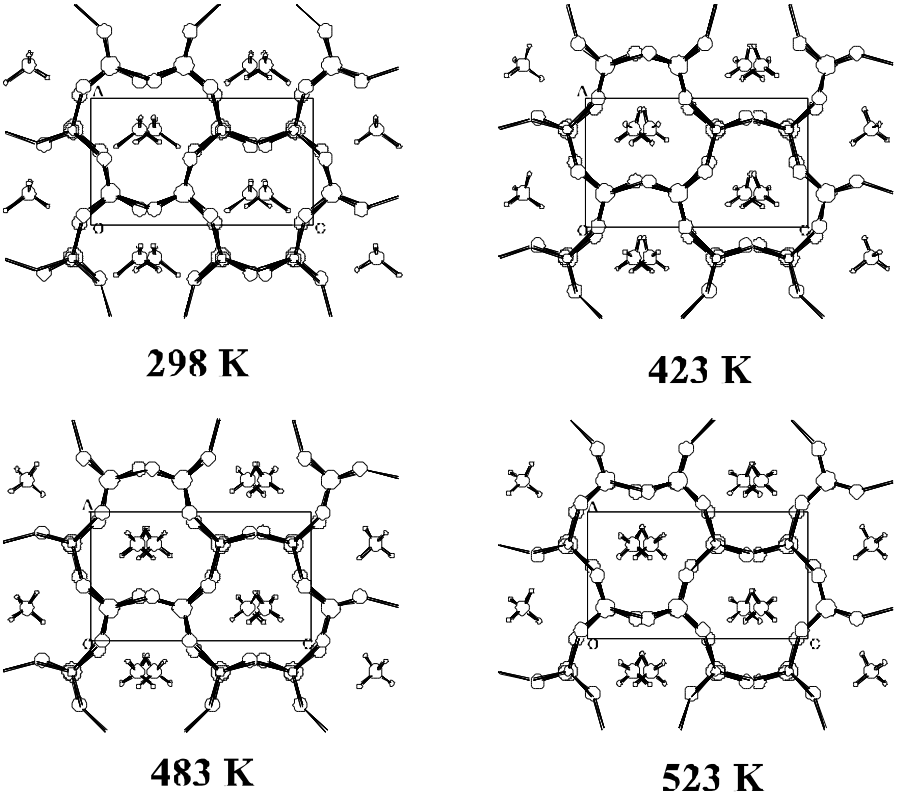

Figure 3. Unit-cell content of $LiNH_4SO_4$ at 298, 423, 483 and 523 K viewed down the *c*-axis.

and *c* parameters practically do not change during the transition at 335 K, but the variation of the slope of the $b(T)$ curve at this temperature suggests the transition.

The transitions are also observed in the Raman spectra. (The heat produced by the laser decreases the transition temperatures in this process). The frequencies of t^{SO_4}, L^{SO_4} and t^{NH_4} in the phase at room temperature change at 323.4 K and these drops when the compound passes to the high-temperature phase (figure 2).

Atomic coordinates of structures at 298, 318, 383, 423 and 483 K, bond lengths and angles and hydrogen bond lengths are listed in tables 4, 5 and 6, respectively. Figure 3 shows a cell projection down the *b*-axis for the structures at 298, 423, 483 and 523 K. The two crystal structures solved here at 298 K are similar to those obtained by Dollase [4]. The main differences are a result of the different number of reflections used in the refinement. Our structures and those described by Dollase have the opposite chirality to those obtained by Mashiyama and Kasano [5], where a chirality test was not carried out.

The crystal structures obtained during the slow warming process show that LAS undergo two phase transitions. We shall give the name phase II to the structure at 298 K, phase II′ at 423 K and phase I′ at 483 K. Phase II′ is produced from phase II by a rotation of the sulphate ion of about 41° around the S–O1 bond and by the displacement of NH_4 ion, practically, along the *a*-axis. This new phase is near to the enantiomeric phase of II. The mixture rate obtained in the refinement of crystal structures at 318 and 383 K shows that the transition was occurred in domains. Phase I′ is produced from phase II′ by a rotation of $-1°$ around the S–O1 bond

Table 4. Atomic coordinates ($\times 10^4$) at different temperatures.

	x	*y*	*z*
298.0 K			
S	2500	2037(1)	4169(1)
O(1)	2422(15)	364(3)	4107(3)
O(2)	1281(7)	2736(3)	2834(4)
O(3)	825(7)	2554(3)	5352(3)
O(4)	5186(7)	2587(3)	4451(3)
N	2492(12)	−33(3)	7847(3)
Li	7430(3)	1768(5)	5881(4)
318.0 K			
S	2500	2031(1)	4164(1)
O(1)	2490(12)	387(2)	4037(3)
O(2)	1568(5)	2714(3)	2813(2)
O(3)	844(5)	2502(3)	5374(2)
O(4)	5094(4)	2566(3)	4457(2)
N	2437(9)	2(2)	7856(2)
Li	7463(19)	1782(4)	5868(3)
383.0 K			
S	2500(7)	2033(1)	4160(1)
O(1)	2536(2)	391(3)	4038(4)
O(2)	3456(9)	2697(4)	2800(3)
O(3)	−62(6)	2572(4)	4473(3)
O(4)	4181(7)	2505(4)	5356(3)
N	2518(13)	5(2)	7868(3)
Li	24 760(4)	−1766(6)	4134(4)
423.0 K			
S	2500	2034(1)	4157(1)
O(1)	2510(3)	395(3)	4037(5)
O(2)	3443(10)	2698(5)	2795(3)
O(3)	−44(8)	2577(4)	4478(4)
O(4)	4206(9)	2510(4)	5343(4)
N	2526(16)	3(3)	7874(3)
Li	2480(4)	−1760(7)	4140(5)
483.0 K			
S	2500	2039(1)	4150(1)
O(1)	2480(3)	408(3)	4039(6)
O(2)	3400(12)	2701(7)	2793(4)
O(3)	−49(9)	2575(5)	4483(5)
O(4)	4215(10)	2514(5)	5317(4)
N	2519(17)	1(3)	7888(3)
Li	2540(4)	−1749(7)	4142(5)
523.0 K			
S	2500	2046(1)	4142(1)
O(1)	2360(4)	428(6)	4030(12)
O(2)	1660(2)	2705(12)	2778(8)
O(3)	740(2)	2527(12)	5259(11)
O(4)	5041(17)	2576(11)	4508(10)
N	2510(3)	−4(5)	7908(6)
Li	2520(6)	−1735(13)	4156(8)

and by the displacement of Li ion. The coordinates obtained for the crystal structure at 298 K, measured after the slow warming process, indicate that the transition at 335 K is reversible.

Table 5. Bond lengths (Å) and angles (°).

	$T = 298.0$ K	$T = 318.0$ K	$T = 383.0$ K	$T = 423.0$ K	$T = 483.0$ K	$T = 523.0$ K
S–O(1)	1.468(3)	1.4471(18)	1.446(2)	1.444(3)	1.434(3)	1.424(6)
S–O(2)	1.507(3)	1.456(2)	1.464(3)	1.461(4)	1.454(3)	1.452(6)
S–O(3)	1.467(3)	1.468(2)	1.467(6)	1.463(3)	1.464(4)	1.449(8)
S–O(4)	1.519(4)	1.472(2)	1.471(4)	1.473(3)	1.465(4)	1.463(8)
O(1)–Li	1.870(6)	1.906(4)	1.896(6)	1.895(6)	1.895(7)	1.902(13)
O(2)–Li [1]	1.932(6)	1.888(4)	1.902(7)	1.903(8)	1.894(8)	1.901(12)
O(3)–Li [2]	1.979(13)	1.946(9)	1.956(14)	1.960(16)	1.936(16)	1.92(3)
O(4)–Li [3]	1.903(10)	1.922(8)	1.921(18)	1.92(2)	1.95(2)	1.94(2)
O(1)–S–O(2)	111.3(2)	109.98(19)	109.1(3)	109.3(3)	109.9(4)	108.6(7)
O(1)–S–O(3)	108.7(2)	109.78(19)	110.5(6)	110.2(6)	109.2(6)	108.0(8)
O(2)–S–O(3)	102.2(2)	108.63(17)	111.0(3)	110.9(2)	110.7(3)	107.4(7)
O(1)–S–O(4)	110.5(3)	109.6(3)	109.3(4)	109.6(4)	109.9(5)	112.3(10)
O(2)–S–O(4)	113.94(17)	109.69(14)	108.0(4)	107.7(3)	107.9(4)	110.8(5)
O(3)–S–O(4)	109.84(17)	109.12(13)	109.0(2)	109.1(2)	109.3(3)	109.5(6)
S–O(1)–Li	176.9(5)	172.8(2)	172.7(4)	172.8(4)	172.9(5)	170.7(12)
S–O(2)–Li [1]	134.6(4)	143.8(3)	142.5(7)	143.0(7)	145.5(8)	146.8(12)
S–O(3)–Li [2]	128.1(2)	129.01(17)	128.9(4)	129.1(4)	128.7(4)	131.6(6)
S–O(4)–Li [3]	125.2(3)	127.8(2)	129.5(3)	129.9(3)	130.5(3)	130.2(8)
O(1)–Li–O(2) [4]	102.7(3)	101.1(2)	01.5(4)	101.6(4)	102.2(4)	101.0(8)
O(1)–Li–O(4) [2]	112.3(5)	113.1(3)	111.4(9)	111.4(10)	109.9(11)	112.8(14)
O(2) [4]–Li–O(4) [2]	110.6(6)	112.5(5)	113.0(6)	112.8(7)	111.6(7)	109.4(12)
O(1)–Li–O(3) [3]	110.6(6)	109.1(5)	112.3(7)	113.0(8)	114.7(8)	114.6(14)
O(2) [4]–Li–O(3) [3]	115.5(4)	111.8(3)	109.4(8)	109.1(9)	110.8(10)	112.5(12)
O(4) [2]–Li–O(3) [3]	105.3(3)	109.00(19)	109.1(3)	108.8(3)	107.6(3)	106.6(7)

Symmetry code: [1] $= x, y + 1/2, -z + 1/2$; [2] $= x - 1/2, -y, -z + 1$; [3] $= x + 1/2, -y, -z + 1$; [4] $= x, y - 1/2, -z + 1/2$.

The crystal structure obtained after the fast warming process shows that LAS underwent only one phase transition. The metastability of phase II in the fast warming process suggests that the transition between phase II and phase II′ is of the first order. We shall give the name phase I to the structure solved at 523 K. Phase I has the same enantiomeric form as phase II, and is produced from phase II by a rotation of 9° around the S–O1 bond and by the displacement of NH_4 and Li ions.

The assignment of non-polar $P2_1nb$ space group in the phases I and I′ is corroborated by the Raman spectra. The main differences between the Raman of the three phases II, II′ and I′ are in the external modes and $\nu_2^{SO_4}$, $\nu_3^{SO_4}$ and $\nu_4^{SO_4}$ modes. The *Pmnb* structure for phase I′, as described by Itoh *et al* [2], consists of a mixture of two enantiomer, one similar to those found for phase II and the second to phase II′, so the $\nu_n^{SO_4}$ frequencies for phase I′ should be a mixture of those observed in the Raman spectra for II and II′, which is not observed in figure 4 and table 3. This is consistent with the assumption of non-disorder structure in the high-temperature phase.

The SO_4 ion was rotated 26.8° (at 298 K) around the S–O1 bond in order to show an hypothetical ordered centrosymmetric structure with space group *Pmnb*. This angle was 17.4° in phase I at 523 K and −19.3° in phase I′ at 483 K. Thus, the angle decreased as temperature increased, suggesting that the ferroelectric–paralectric transition is a displacive transition.

The SO_4 ion has C_{2h} symmetry at 298 K, with two short and two long S–O bonds, while it shows a C_{3h} symmetry in phases II′, I′ and I. This is also observed in the stretching $\nu_n(SO_4)$ modes (figure 4 and table 3). The shortest S–O bond length corresponded to the O atom

Table 6. Hydrogen bond lengths (Å) at different temperatures.

298 K		423 K	
N–H1. . .O2 [2]	3.162(6)	N–H1. . .O4 [4]	2.872(6)
N–H2. . .O3 [3]	2.819(5)	N–H2. . .O2 [3]	2.962(8)
N–H2. . .O4 [4]	2.867(5)	N–H2. . .O3 [5]	2.886(6)
N–H3. . .O1 [1]	3.227(9)	N–H3. . .O1 [1]	3.202(15)
N–H3. . .O4 [1]	3.300(5)	N–H4. . .O1 [2]	3.188(15)
N–H4. . .O2 [5]	2.838(6)	N–H4. . .O3 [5]	2.886(6)
318 K		483 K	
N–H1. . .O3 [4]	2.850(4)	N–H1. . .O4 [4]	2.877(6)
N–H2. . .O4 [3]	2.867(4)	N–H2. . .O2 [3]	2.974(9)
N–H3. . .O1 [1]	3.149(7)	N–H2. . .O3 [5]	2.885(7)
N–H4. . .O1 [2]	3.196(7)	N–H3. . .O1 [1]	3.224(16)
N–H4. . .O2 [5]	2.962(5)	N–H3. . .O2 [1]	3.284(9)
		N–H4. . .O1 [2]	3.189(16)
383 K		N–H4. . .O3 [5]	2.885(7)
N–H1. . .O4 [4]	2.869(5)		
N–H2. . .O2 [3]	2.952(7)	523 K	
N–H2. . .O3 [5]	2.885(6)	N–H1. . .O3 [4]	2.900(13)
N–H3. . .O1 [1]	3.183(11)	N–H2. . .O4 [3]	2.899(14)
N–H4. . .O1 [2]	3.199(11)	N–H3. . .O1 [1]	3.28(2)
N–H4. . .O3 [5]	2.885(6)	N–H4. . .O1 [2]	3.15(2)
		N–H4. . .O2 [5]	2.984(17)

Symmetry code: [1] $= x-1/2, -y, 1-z$; [2] $= x+1/2, -y, 1-z$; [3] $= x-1/2, 1/2-y, 1/2+z$; [4] $= x, y-1/2, 3/2-z$; [5] $= 1/2+x, 1/2-y, 1/2+z$.

with weakest N . . . O hydrogen bond and the shortest Li–O length, which is in agreement with the assumption of higher electron localization in O1. This has also been observed in $(NH_4)_{2-x}K_xSO_4$ mixed crystals [12] and $(NH_4)_{2-x}K_xSeO_4$ [13, 14].

Table 7. Spontaneous polarization versus the temperature, which has been computed from the atomic coordinates by using an ionic model.

$T(K)$	$P \times 10^6$ (C cm^{-2})
293	0.26(4)
423	0.42(4)
483	0.03(4)
523	0.04(6)

The SO_4 tetrahedron shared all of its corners with LiO_4 tetrahedra and vice versa, giving a tetrahedral framework. The NH_4 ions lay approximately in the centre of the large asymmetric cavities in the framework, giving single or bifurcated hydrogen bonds with the oxygen atoms. At 298 K the hydrogen bonds with H1 and H3 were weak (average N . . . O bond length 3.21 Å), while those with H2 and H4 were stronger (2.84 Å). As the temperature increased N stretched to produce three strong hydrogen bonds and only one weak bond. This meant that the average N . . . O bond length was 3.03 Å at 298 K becoming 2.96–2.97 Å in the crystal structures at 318, 383 and 423 K. This average value however returned to growth in the transition from phase II or II′ to I or I′ (average values 3.02 Å at 483 K and 3.04 Å at 523 K).

We used an ionic model to compute the spontaneous polarization in each structure; the

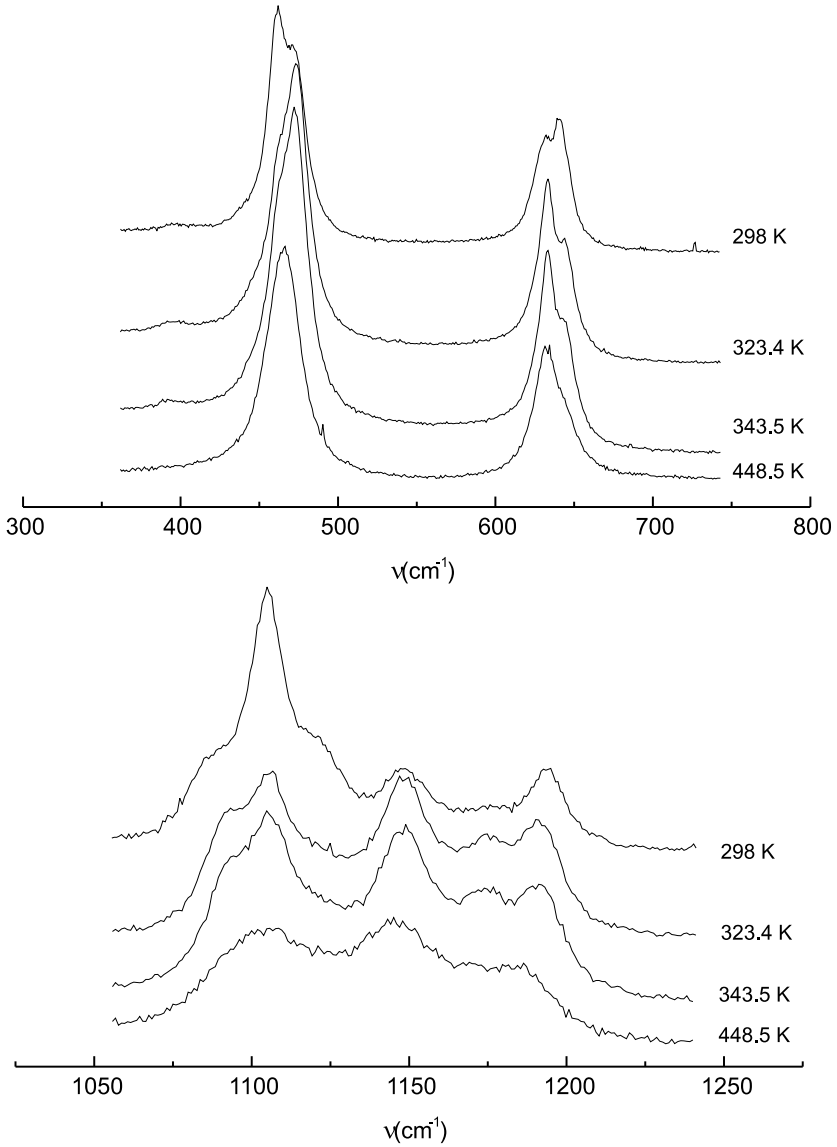

Figure 4. $\nu_2^{SO_4}$, $\nu_3^{SO_4}$ and $\nu_4^{SO_4}$ modes of LAS at different temperatures.

values obtained are shown in table 7. The spontaneous polarization along the x-axis was equal to:

$$\boldsymbol{P} = \Sigma \boldsymbol{x}_i q_i$$

where q_i is the charge of the ion i and $\boldsymbol{x}_i$ is the atomic displacement of the atom along the polarization axis. The solution of equation $0 = \Sigma \boldsymbol{x}_i q_i$ with the neutrality condition $0 = \Sigma q_i$ offers a trivial solution: for each value $\boldsymbol{x}_i$ there exists a j coordinate with $q_i = q_j$ where $\boldsymbol{x}_i = -\boldsymbol{x}_j$. This solution gives a non-polar space group of symmetry, but other combinations of $\boldsymbol{x}_i$ values lead to the removal of the spontaneous polarization depending on the number of terms in the equation.

4. Conclusions

We structurally characterized the phases of $LiNH_4SO_4$ in the temperature range 298–600 K. The framework of corner-shared LiO_4 and SO_4 tetrahedra is relatively flexible, producing large asymmetric cavities, in which the ammonium ions are located. The number of phases was dependent on the rate of the warming process. If a warming rate of 5 K min^{-1} is used, from the $P2_1nb$ structure (phase II), stable at room temperature, is obtained a new phase above 335 K (phase II′), which is close to the enantiomeric form of phase II and a paraelectric (with spontaneous polarization equal to 0) phase I′ above 461 K, which shows the non-polar $P2_1nb$ space group. A warming rate of 20 K min^{-1} gave directly the paraelectric phase I above 461 K. Phase I is close to the enantiomeric form of phase I′.

Acknowledgment

The authors thank the Comisión Interministerial de Ciencia y Tecnología for financial support through grant MAT97-0371.

References

[1] Kruglik I, Simonov M A and Aleksandrov K S 1978 *Kristallografiya* **23** 494
[2] Itoh K, Ishikura H and Nakamura E 1981 *Acta Crystallogr.* B **37** 664
[3] Lukaszewicz K and Pietraszko A 1992 *Pol. J. Chem.* **66** 2057
[4] Dollase A 1969 *Acta Crystallogr.* B **25** 2298
[5] Mashiyama H and Kasano H 1993 *J. Phys. Soc. Japan* **62** 155
[6] Polomska M, Hilezer B and Baran J 1994 *J. Mol. Struct.* **325** 105
[7] Torgashev V I, Yuzyuk Yu I, Smutny F and Polomska M 1988 *Sov. Phys. Crystallogr.* **33** 700
[8] Sheldrick G M 1997 *SHELXS. A Computer Program for Crystal Structure Determination* University of Göttingen
[9] Sheldrick G M 1997 *SHELXL, A Computer Program for Crystal Structure Determination* University of Göttingen
[10] Flack H D 1983 *Acta Crystallogr.* A **39** 867
[11] Rodríguez-Carvajal J 1996 *FULLPROF* version 3.1c, Laboratoire Leon Brillouin, Paris
[12] González-Silgo C, Solans X, Ruiz-Pérez C, Martínez-Sarrión M L, Mestres L and Bocanegra E 1997 *J. Phys.: Condens. Matter* **9** 2657
[13] González-Silgo C, Solans X, Ruiz-Pérez C, Martínez-Sarrión M L and Mestres L 1996 *Ferroelectrics* **177** 191
[14] Solans X, Ruiz-Pérez C, González-Silgo C, Mestres L, Martínez-Sarrión M L and Bocanegra E 1998 *J. Phys.: Condens. Matter* **10** 5245